RSC Advances

PAPER

Cite this: *RSC Adv.*, 2016, **6**, 88979

Phosphonium ionic liquids as greener electrolytes for poly(vinyl chloride)-based ionic conducting polymers†

A. M. A. Dias,[a] S. Marceneiro,[a] H. D. Johansen,[b] M. M. Barsan,[b] C. M. A. Brett*[b] and H. C. de Sousa*[a]

Ionic liquid based ion-conducting polymers have been prepared and characterized by loading poly(vinyl chloride) (PVC) with one of two phosphonium-based ionic liquids (PhILs) (trihexyl(tetradecyl) phosphonium bis(trifluoromethylsulfonyl)imide, $[P_{14,6,6,6}][Tf_2N]$ and trihexyl(tetradecyl) phosphonium chloride, $[P_{14,6,6,6}][Cl]$) and a commonly used PVC plasticizer (di-isononyl phthalate, DINP). Different proportions of each charged (PhILs) and non-charged (DINP) additive were used to evaluate the influence of PhIL ionicity on the ionic conductivity of the PVC-based electrolyte and to study the effect of the thermomechanical properties of PVC on the diffusivity of ionic charges in between PVC molecular chains, and consequently on the electrochemical properties of the polymer. Films were characterized for their chemical, morphological, thermomechanical and electrical properties. The results show that both PhIL ionicity and PhIL–PVC compatibility play a major role in decreasing the electrical resistivity of PVC films. The lowest film resistivity (0.4 kΩ cm), corresponding to an estimated electrical conductivity of ~2.4 μS cm^{-1}, was observed for PVC films loaded with the highest tested amount of $[P_{14,6,6,6}][Tf_2N]$ (45 wt% of PhIL at fixed DINP composition, 9 wt%). These films were also stable at temperatures up to 200 °C without using any further PVC thermal stabilizer. The polymer electrolytes presented in this work may be used as platforms to produce soft, safer and cost-effective ion-conducting materials by using non-volatile and electrochemically stable PhILs as liquid electrolytes incorporated into a cheap, stable and versatile polymer such as PVC.

Received 4th June 2016
Accepted 7th September 2016

DOI: 10.1039/c6ra14528k

www.rsc.org/advances

Introduction

Gel polymer electrolytes are ionically conducting polymers which are being extensively studied as promising materials for both electrochemical (electric double layer capacitors, super capacitors, sensors, and flexible electronics) and electromechanical (actuators) applications, mostly due to their inherent properties such as shape versatility, flexibility, light weight and processability.[1,2] These materials are composed of a polymer (*e.g.* poly(ethylene oxide) and copolymers of poly(vinylidene fluoride)), a high-dielectric solvent and/or plasticizer, and highly conductive inorganic salts, thus combining the mechanical stability of the polymer network with the high conductivity of the electrolytes entrapped in the solid matrix. Although gelled electrolytes maintain their mechanical stability for longer actuation periods, they still present safety and efficiency concerns related to solvent and/or plasticizer volatility/leaching, corrosiveness, flammability and/or toxicity as well as generally low ionic conductivities.[3]

In recent years, room temperature ionic liquids (RTILs) have been proposed as greener alternatives to conventional electrolytes since they present large electrochemical potential windows (from 5.0 to 6.0 V amplitude owing to their ionic nature),[4–6] near-zero volatility (below 1 Pa at 25 °C, which avoids leakage due to evaporation), non-flammability and high thermal and chemical stability.[7,8] Another major advantage of RTILs over conventional inorganic electrolytes is their task-specific and tailor-made capacities that permit tuning their physicochemical properties by the judicious conjugation of specific cations and anions. This feature has favoured the widespread use of RTILs as multifunctional additives for different natural and synthetic-based polymer matrices.[9–11]

Poly(vinyl chloride) (PVC) is one of the most important commodity polymers with widespread applications in different fields due to its low cost, transparency, durability, chemical resistance, biocompatibility, processability and compatibility with a variety of additives that can improve its mechanical,

[a]*CIEPQPF, Chemical Engineering Department, Faculty of Sciences and Technology, University of Coimbra, Rua Sílvio Lima, Pólo II – Pinhal de Marrocos, 3030-790 Coimbra, Portugal. E-mail: hsousa@eq.uc.pt; Fax: +351-239-798703; Tel: +351-239-798700*

[b]*Department of Chemistry, Faculty of Sciences and Technology, University of Coimbra, 3004-535 Coimbra, Portugal. E-mail: cbrett@ci.uc.pt; Fax: +351-239-827703; Tel: +351-239-854470*

† Electronic supplementary information (ESI) available. See DOI: 10.1039/c6ra14528k

Table 1 Comparison of some physico-chemical properties of trihexyltetradecylphosphonium chloride ($[P_{14,6,6,6}][Cl]$) and trihexyltetradecylphosphonium bis(trifluoromethylsulfonyl)imide ($[P_{14,6,6,6}][Nf_2T]$)

PhIL	M_w (g mol^{-1})	V_m[a] (25 °C) (cm^3 mol^{-1})	x_{free}[a] (25 °C) V_{free}/V_m	η[b] (40 °C) (Pa s)	σ[b] (40 °C) (S cm^{-1})	T_g[c] (°C)
$[P_{14,6,6,6}][Cl]$	519.31	582.74	0.09–0.12	0.70	9.5×10^{-6}	−57.9
$[P_{14,6,6,6}][Nf_2T]$	764.01	716.30	0.11–0.14	0.15	1.8×10^{-4}	−70.8

[a] At the molecular level, the free volume V_{free} which is defined as the difference between the volume of an ion pair V_{pair} (the total mass of the ion pair divided by the experimental liquid density) and the sum ($V^+ + V^-$) of the cation and anion volumes.[21] [b] Fraser *et al.*, 2007.[22] [c] This work.

physical and chemical properties. PVC gels have also been shown to possess unique deformation capacity when subjected to an electrical field and have therefore been proposed as a platform for the development of different types of electro-actuators.[12–14] However, actuation was only achieved at high DC voltages, which limits their broad application.[15,16] In a previous study, Hirai and co-authors doped PVC gels with different phosphonium based RTILs (PhILs), which were used to improve the actuation behaviour of PVC gels in low electrical fields.[17] The authors reported that trihexyl(tetradecyl) phosphonium chloride ($[P_{14,6,6,6}][Cl]$) was the most compatible with PVC and the resulting gels showed improved actuation, higher dielectric constant and lower interfacial resistance (compared to PVC gel without PhIL), even for a low incorporated amount of PhIL (0.01 wt%). Nevertheless, halogenated based RTILs are able to induce the thermal degradation of PVC, even under mild temperature conditions[10,18,19] which may limit the use of this type of RTILs in the development of ion-conducting PVC-based solid electrolytes. On the contrary, RTILs with the $[Tf_2N]^-$ anion present the highest thermal stability (independently of the cation type),[19] and $[P_{14,6,6,6}][Tf_2N]$ in particular has been shown to significantly improve the thermal stability of both suspension and emulsion grades of PVC.[10,20] Moreover, and as can be seen in Table 1, the ionic conductivity of $[P_{14,6,6,6}][Tf_2N]$ is higher than that of the halogenated equivalent $[P_{14,6,6,6}][Cl]$, despite the fact that the $[Tf_2N]^-$ anion is bulkier than $[Cl]^-$. This occurs due to strong ion-pairing or ion-association in $[P_{14,6,6,6}][Cl]$ owing to the small size of the halide anion enabling it to be closely bonded to the positively charged cation.[22,23] The bulkier and asymmetric bis(-trifluoromethylsulfonylimide) anion hinders the formation of stable ion pairs so that cation and anion charge diffusion are independent for $[P_{14,6,6,6}][Tf_2N]$.[4,22,24,25]

The conduction efficiency of ion-conducting solid materials depends on the number of unpaired ionic charge carriers, and thence on the ionicity of the electrolyte and on ion diffusivity within the solid support, which in turn depends on the structure of the solid matrix as well as on the strength of structure–ion interactions.[26] Recent studies have reported the advantages of RTIL/polymer microphase segregation on improving the ionic conductivity of polymer electrolytes. The efficiency of these systems results from the formation of an ion-conducting domain (RTIL rich phase) dispersed within a polymeric network which facilitates ion diffusion while providing mechanical robustness and thermal stability.[27–29] Interestingly, our group has previously observed $[P_{14,6,6,6}][Tf_2N]$/PVC microphase segregation, at RTIL concentrations higher than 10 wt%, due to electrostatic repulsion between the highly electronegative chlorine and fluorine atoms from the PVC matrix and the PhIL anion, respectively[10] and also to the lower hydrogen-bond-accepting capacity of the $[Tf_2N]^-$ anion compared to that of the chloride anion.[19]

Therefore, and based on all this evidence, the present work aims to compare the efficiency of $[P_{14,6,6,6}][Cl]$ and $[P_{14,6,6,6}][Tf_2N]$ as non-volatile and non-flammable greener electrolytes for the development of safer, soft, processable, versatile and low cost PVC based ion-conducting materials. Phosphonium-based ILs were used because they are cheaper, commercially available in large quantities, and present lower toxicity, higher chemical and thermal stability and a larger potential window than most ILs.[5,30–32] Furthermore, and in order to study the effect of inter-chain free volume and polymer chain mobility on the diffusivity of ionic charges confined between PVC molecular chains, the conventional plasticizer diisononyl phthalate (DINP) was also used as additive due to its already-proved PVC plasticizing efficiency and high thermal stability, at relatively low cost.[33] Although phthalate-based plasticizers have been identified as compounds that may present some health risks, such risks depend on the type and duration of exposure to the phthalate plasticized material. Previously reported results showed that PVC films loaded with up to 20% wt of DINP did not present haemolytic activity or toxicity against differentiated human Caco-2 cells and HepG2 cells.[10]

The materials were synthesized using different proportions of commodity chemicals (polymer and additives) and conventional easy-to-apply film casting procedures, and were characterized with respect to their morphology and homogeneity, hydrophilicity, thermomechanical stability and electrochemical response (impedance spectroscopy). These materials are envisaged as platforms for the design of soft electronic and robotic devices such as sensors, power sources and electroactuators with potential use in biomedical applications such as bio-actuators, biosensors and electro-responsive drug delivery.

Materials and methods

Chemicals

Phosphonium-based ionic liquids (PhILs), namely trihexyl(tetradecyl) phosphonium bis(trifluoromethylsulfonyl)imide ($[P_{14,6,6,6}][Tf_2N]$) and trihexyl(tetradecyl) phosphonium chloride ($[P_{14,6,6,6}][Cl]$) were supplied by Cytec Industries, Canada, with purities higher than 99%. Biomedical grade suspension poly(vinyl chloride) (PVC) powder (VICIR S2000, M_n = 91 kg

mol^{-1} with $M_w/M_n = 1.7$, apparent density = 0.42–0.50 g cm^{-3}, *K*-value = ~80) was supplied by Companhia Industrial de Resinas Sintéticas, CIRES, S.A., Portugal. GC grade tetrahydrofuran (THF, purity > 99%) and di-isononyl phthalate (DINP, purity > 99%) were obtained from Sigma-Aldrich.

Preparation of PhIL/DINP loaded PVC films

PVC samples, with and without additives, were prepared by solvent casting. PVC was initially dissolved in THF (5% (w/v)). After 24 h stirring, different amounts of each of PhIL and/or DINP were added to the initial PVC/THF solutions in order to obtain different final PVC/PhIL/DINP compositions, as indicated in Table 2. The samples were identified as PhIL type/PhIL amount (wt)/DINP amount (wt) where PhIL refers to trihexyl(tetradecyl) phosphonium chloride ($[P_{14,6,6,6}][Cl]$) or trihexyl(tetradecyl) phosphonium bis(trifluoromethylsulfonyl)imide ($[P_{14,6,6,6}][Tf_2N]$). The mixtures were stirred for 8 h, poured into Petri dishes and left to evaporate for one week in a saturated THF environment in order to obtain homogeneous films. Films were then dried in a vacuum oven (at 40 °C) until constant weight. Film thicknesses were measured using a digital micrometer (Mitutoya, model MDC-25S, Japan).

Characterization of the films

Morphological characterization. A scanning electron microscope (SEM), coupled to energy dispersive X-rays (Phillips, EDX Genesis, model XL 30) was used to analyse the surface morphologies of the films as well as the spatial distribution and homogeneity of the PhILs in the prepared PVC films. SEM-EDX micrographs were obtained at 10 kV for gold-sputtered samples (300 Å).

Light transmittance. Transmittance of UV and visible light through samples of size 1 × 3 cm^2 placed on the inner wall of a quartz cell, was measured in duplicate from 200 to 900 nm using a UV-Visible spectrophotometer (Jasco, model 560, Japan) at room temperature.

Water contact angles. Static contact angle measurements were performed using Milli-Q water, at room temperature (20–23 °C), and employing the sessile-drop method (Dataphysics Instruments, OCA 20, Germany). The volume of the drop was equal to 10 μL and the measurements were repeated in triplicate.

Thermomechanical behaviour. The thermal stability of the samples was determined by thermogravimetric analysis (TGA) using a Thermogravimetric Analyzer (TA Instruments, Q500, USA). Experiments were carried out from room temperature up to 600 °C, at a heating rate of 10 °C min^{-1}, under a dry nitrogen atmosphere (flow rate 40 mL min^{-1}) and using samples with an average mass of 6.5 ± 1.5 mg. The elastic modulus and the glass transition temperatures (T_g) of the films was measured by dynamic mechanical thermal analysis (DMTA) using the tension mode at 1, 5 and 10 Hz and with a displacement of 0.05 mm (Triton, Tritec 2000, UK). The temperature profile was obtained at 2 °C min^{-1} heating rate (from −180 °C up to 110 °C) with a time delay of 1 s. The glass transition temperatures were determined as the peak in the damping factor curve (tan $\delta = E''/E'$, where E'' and E' are the loss and the storage modulus, respectively). The T_g of the pure PhILs was measured in the single cantilever, with the liquids inserted into a stainless steel pocket, using the same operating conditions described above.

Impedance spectroscopy measurements. Electrochemical impedance spectroscopy (EIS) experiments were carried out using a PGSTAT 30 potentiostat–galvanostat with a Frequency

Table 2 Composition of the PVC/PhIL/DINP films prepared by solvent casting. Samples are identified according to the following code PhIL type/PhIL composition (wt)/DINP composition (wt) were PhIL refers to trihexyl(tetradecyl) phosphonium chloride ($[P_{14,6,6,6}][Cl]$) or to trihexyl(tetradecyl) phosphonium bis(trifluoromethylsulfonyl)imide, ($[P_{14,6,6,6}][Tf_2N]$)

Sample	PVC (g)	$[P_{14,6,6,6}][Cl]$ (g)	$[P_{14,6,6,6}][Tf_2N]$ (g)	DINP (g)	PhIL + DINP wt (%)	Thickness (mm)	Transmittance[a] (%)	Water contact angle (°)
Increasing DINP at fixed incorporated amount of PhIL								
$[P_{14,6,6,6}][Cl]$/0.15/0	0.75	0.15	—	—	16.7	0.264 ± 0.002	42.30 ± 0.28	87.82 ± 1.81
$[P_{14,6,6,6}][Cl]$/0.15/0.25			—	0.25	34.8	0.321 ± 0.004	55.73 ± 3.77	92.64 ± 2.30
$[P_{14,6,6,6}][Cl]$/0.15/0.50			—	0.50	46.4	0.311 ± 0.003	76.77 ± 2.98	92.20 ± 2.63
$[P_{14,6,6,6}][Cl]$/0.15/0.75			—	0.75	54.5	0.369 ± 0.010	88.42 ± 2.02	99.79 ± 1.47
$[P_{14,6,6,6}][Tf_2N]$/0.15/0	0.75	—	0.15	—	16.7	0.260 ± 0.003	74.60 ± 0.60	81.05 ± 2.99
$[P_{14,6,6,6}][Tf_2N]$/0.15/0.25		—		0.25	34.8	0.280 ± 0.003	85.92 ± 3.95	104.51 ± 3.36
$[P_{14,6,6,6}][Tf_2N]$/0.15/0.50		—		0.50	46.4	0.361 ± 0.001	84.98 ± 0.66	102.46 ± 3.16
$[P_{14,6,6,6}][Tf_2N]$/0.15/0.75		—		0.75	54.5	0.419 ± 0.003	80.13 ± 3.85	94.83 ± 0.33
Increasing PhIL at fixed incorporated amount of DINP								
PVC/0/0.15	0.75	—	—	0.15	16.7	0.283 ± 0.002	83.48 ± 0.90	80.54 ± 2.86
$[P_{14,6,6,6}][Cl]$/0.25/0.15	0.75	0.25	—	0.15	34.8	0.288 ± 0.001	74.44 ± 3.44	87.99 ± 2.75
$[P_{14,6,6,6}][Cl]$/0.50/0.15		0.50	—		46.4	0.357 ± 0.013	83.67 ± 3.45	51.93 ± 0.98
$[P_{14,6,6,6}][Cl]$/0.75/0.15		0.75	—		54.5	0.373 ± 0.001	71.64 ± 5.44	49.62 ± 0.69
$[P_{14,6,6,6}][Tf_2N]$/0.25/0.15	0.75	—	0.25	0.15	34.8	0.299 ± 0.004	79.65 ± 1.67	91.11 ± 0.62
$[P_{14,6,6,6}][Tf_2N]$/0.50/0.15		—	0.50		46.4	0.392 ± 0.007	83.64 ± 2.62	95.96 ± 1.00
$[P_{14,6,6,6}][Tf_2N]$/0.75/0.15		—	0.75		54.5	0.401 ± 0.013	75.13 ± 4.86	99.02 ± 2.23

[a] Measured at 600 nm.

Response Analyser (FRA2) module controlled by FRA software version 4.9 (EcoChemie, Utrecht, Netherlands). A rms perturbation of 350 mV was applied over the frequency range between 1.0 MHz and 0.1 Hz (ten frequency values per decade). PVC films loaded with different amounts of PhILs and/or DINP were sandwiched between two blocking electrodes (1 cm^2, S136 steel) in the measurement cell, in air. Spectra were recorded at 0.10 V, applied between the two electrodes, and the spectra were fitted using electrical equivalent circuits (ZView 3.2 software, Scribner Associates Inc., USA).

Results and discussion

Morphological characterization

Poly(vinyl chloride) films prepared with variable amounts of the ionic liquids trihexyl(tetradecyl) phosphonium chloride ($[P_{14,6,6,6}][Cl]$) or trihexyl(tetradecyl) phosphonium bis(trifluoromethylsulfonyl)imide ($[P_{14,6,6,6}][Tf_2N]$) and di-isononyl phthalate (DINP), were first analyzed for their uniformity and morphological characteristics. The films obtained were homogeneous with no visual detection of surface irregularities (macroscopic visual aspect). The film thicknesses varied according to the composition of the films and ranged between 0.26 and 0.42 mm, increasing with the incorporated amount of PhIL or DINP (Table 2). The transparency of the films was also evaluated by measuring their transmittance at 600 nm to indirectly access polymer–plasticizer compatibility and miscibility.

The results presented in Table 2 indicate that, at fixed incorporated amount of PhIL, the transparency of the films increases on increasing the amount of DINP, from ~40% up to 90% for samples $[P_{14,6,6,6}][Cl]$/0.15/0 and $[P_{14,6,6,6}][Cl]$/0.15/0.75, respectively and from ~75% up to 85% for samples $[P_{14,6,6,6}][Tf_2N]$/0.15/0 and $[P_{14,6,6,6}][Tf_2N]$/0.15/0.75, respectively. The significant increase observed for films loaded with $[P_{14,6,6,6}][Cl]$ may be due to a color dilution effect caused by DINP, since films loaded with only $[P_{14,6,6,6}][Cl]$ are translucent with a brown color. The transmittance of the films at 800 nm (where no colour effects are detected) is higher than 80% for all the compositions tested (data not shown). Therefore, the low transmittance of these films at 600 nm is due to colour effects and not to polymer–$[P_{14,6,6,6}][Cl]$ miscibility issues. A similar effect was previously reported for PVC films loaded with two other phosphonium halides, namely tetrabutyl phosphonium bromide ($[P_{4,4,4,4}][Br]$) and tetrabutyl phosphonium chloride ($[P_{4,4,4,4}][Cl]$).[10] At fixed incorporated amount of DINP, the transparency decreases for PhIL/0.25/0.15 and PhIL/0.75/0.15 samples (<15% for both PhILs), indicating the existence of PVC–PhILs–DINP immiscibility at these compositions. This effect is more evident for $[P_{14,6,6,6}][Tf_2N]$/0.75/0.15 samples, which are opaque white.

SEM-EDX analysis confirmed these results, as shown in Fig. 1. As can be seen, there is clear evidence of phase segregation in sample $[P_{14,6,6,6}][Tf_2N]$/0.75/0.15, with the formation of cavities at the surface of the film due to exudation of $[P_{14,6,6,6}][Tf_2N]$. It was not possible to analyze the cross section of the films, in order to confirm the existence of similar cavities through the entire PVC matrix, because the films were very ductile, which made it difficult to cut them without damaging the structure. On the contrary, and although the surface of the sample $[P_{14,6,6,6}][Cl]$/0.75/0.15 shows a higher roughness than that of films plasticized only with DINP, there is no evidence of $[P_{14,6,6,6}][Cl]$ segregation, even considering its higher viscosity compared to that of $[P_{14,6,6,6}][Tf_2N]$ (Table 1).

The homogeneity of the distribution of each PhIL over the surface of the PVC matrix was analyzed by SEM-EDX. The cation was identified by the element phosphorus, while the anions were identified by the elements chlorine (for $[P_{14,6,6,6}][Cl]$) and sulphur (for $[P_{14,6,6,6}][Tf_2N]$). The distribution of chlorine was normalized in order to eliminate the effect of the signal from chlorine atoms present in the PVC structure. The images show a uniform distribution of all the analyzed elements over the area analysed (60 × 60 μm^2) that includes the film surface and cavities, without the presence of agglomerates, even for the sample loaded with $[P_{14,6,6,6}][Tf_2N]$, and despite the occurrence of segregation.

Water contact angle

The effect of the additives on the hydrophilicity of the samples was investigated by static water contact angle (WCA) measurements. The results (Table 2) showed that the hydrophobicity of the films increases with the added amount of plasticizer (at fixed $[P_{14,6,6,6}][Cl]$ or $[P_{14,6,6,6}][Tf_2N]$ composition) or $[P_{14,6,6,6}][Tf_2N]$ (at fixed plasticizer composition). For higher amounts of incorporated $[P_{14,6,6,6}][Tf_2N]$ or DINP, the hydrophobicity of the films is higher than that previously reported for neat PVC (86.64 ± 1.27°).[10] On the contrary, the hydrophobicity of the films significantly decreases (up to 38%) with an increase in the amount of $[P_{14,6,6,6}][Cl]$, for a fixed amount of plasticizer. Overall, these results indicate that it is possible to tune the hydrophobicity of the PVC films by incorporation of a different type or amount of PhILs and/or DINP. This is a very important aspect, since surface hydrophobicity and wettability may condition the applicability of these conductive materials.[34] For instance, if they are envisaged for the design of actuators for biomedical applications, surface properties may influence the materials' biocompatibility since highly hydrophilic surfaces are known to promote cell adhesion while hydrophobic surfaces may lead to protein adsorption and denaturation.[35] Moreover, a higher hydrophilicity will be favourable for the development of proton exchange conductive membranes which are largely dependent on the amount of water retained by the solid matrix (and which depends on its hydrophilicity) to achieve higher proton conduction.[11,36]

Thermal stability

The thermal stability of the films was analysed by TGA and the results are presented in Fig. 2 and Table 3. The thermogram obtained for neat PVC is also shown for comparison. There is an initial weight loss that starts at ~80 °C, probably due to polymer chain reorganization after dissolution in THF, followed by two major degradation events at ~273 °C and 455 °C due to HCl elimination with the formation of a polyene and to C–C scission, respectively. According to Fig. 2A, and from the profiles

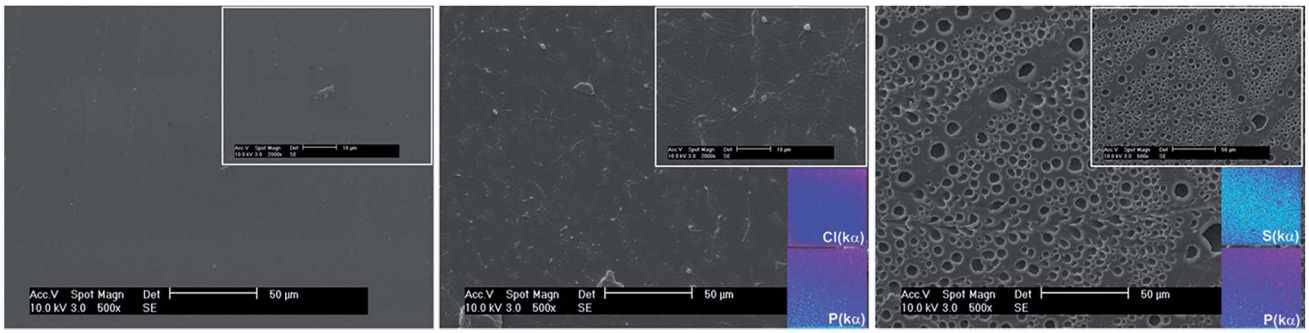

Fig. 1 Micrographs (at different magnifications) of PVC/PhIL/DINP samples: (a) PVC/0/0.15 (PVC films plasticized only with DINP); (b) $[P_{14,6,6,6}][Cl]/0.75/0.15$ and (c) $[P_{14,6,6,6}][Tf_2N]/0.75/0.15$. Inner figures in (b) and (c) present the elemental mapping of phosphorus (P), chlorine (Cl) and sulphur (S) Kα element emissions obtained from EDX elemental analysis. Images were taken from arbitrary sampling areas of 60 × 60 μm^2.

obtained for the films loaded only with PhILs, it can be clearly seen that $[P_{14,6,6,6}][Tf_2N]$ improves the thermal stability of the films more than $[P_{14,6,6,6}][Cl]$. Films loaded with $[P_{14,6,6,6}][Tf_2N]$ also present higher thermal stability than neat PVC. This is in agreement with previously reported data which refer to the outstanding thermal stability of phosphonium based RTILs in general and of the bis(trifluoromethylsulfonyl)imide ($[Tf_2N]^-$) anion in particular.[10,22,37] It also confirms the advantage of the incorporation of this PhIL into polymers whose applicability requires thermal stability at temperatures up to 150 °C, since it avoids the use of PVC thermal stabilizers. Above this temperature, films start to lose weight; however, the weight losses at 200 °C for samples loaded with the minimum $[P_{14,6,6,6}][Tf_2N]$ loaded amount are less than 1.7%, which may be acceptable, depending on the final application. At fixed PhIL composition, the incorporation of DINP slightly improves the thermal stability of the films loaded with $[P_{14,6,6,6}][Tf_2N]$ and $[P_{14,6,6,6}][Cl]$, although, in the latter case, the thermal stability is guaranteed only up to 150 °C (the weight loss of sample $[P_{14,6,6,6}][Cl]/0.15/0.75$ at 150 °C is 1%).

At fixed plasticizer composition, on increasing the amount of $[P_{14,6,6,6}][Tf_2N]$, the films maintain their thermal stability up to 200 °C. The results are even slightly better than those presented above, with weight losses at 200 °C less than 0.7%, although no significant difference, compared with samples loaded only with DINP, was observed at the temperatures at which degradation starts to occur (T_{on} and T_p values). On the contrary, an increase in the amount of $[P_{14,6,6,6}][Cl]$ leads to a significant decrease of the thermal stability of the films, which is even lower than that observed for non-loaded PVC (a decrease in the values of T_{on}, T_p, $T_{10\%}$ and an increase in the weight loss at 200 °C, see Table 3) (Fig. 2B). These results confirm the dehydrochlorination catalytic capacity previously reported for ILs containing chloride anions despite the cation type/size.[10,18]

Thermomechanical analysis

Polymer plasticization is one of the most effective approaches to achieve a desirable enhancement in polymer electrolyte conductivity. The incorporation of low molecular weight additives into the polymer electrolyte structure helps to enhance its

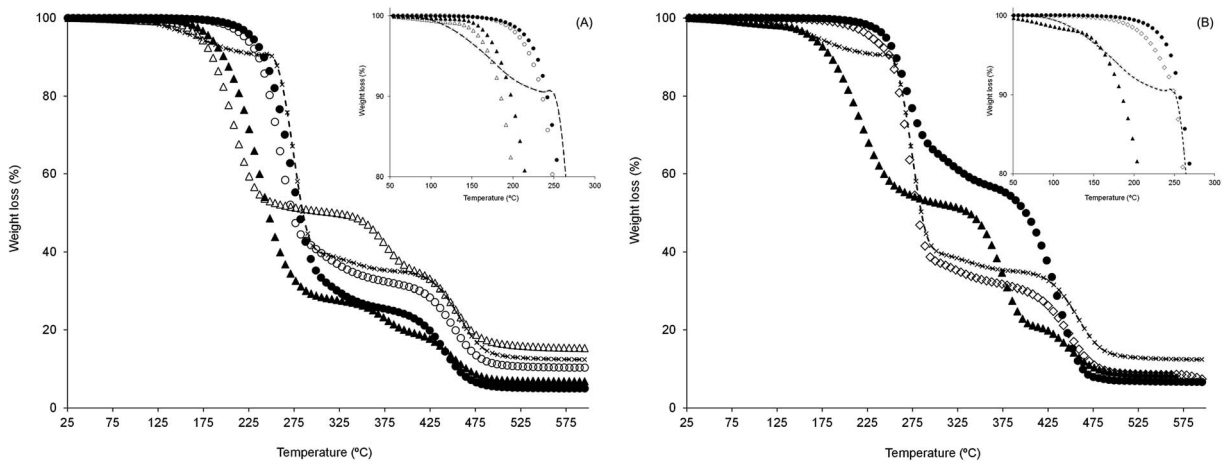

Fig. 2 Thermal stability and degradation profiles of prepared PVC/PhIL/DINP films. (A) Effect of DINP at fixed PhIL composition: (△) $[P_{14,6,6,6}][Cl]/0.15/0$; (▲) $[P_{14,6,6,6}][Cl]/0.15/0.75$; (○) $[P_{14,6,6,6}][Tf_2N]/0.15/0$ and (●) $[P_{14,6,6,6}][Tf_2N]/0.15/0.75$. (B) Effect of PhILs at fixed DINP composition: (□) PVC/0/0.15; (▲) $[P_{14,6,6,6}][Cl]/0.75/0.15$ and (●) $[P_{14,6,6,6}][Tf_2N]/0.75/0.15$. Dashed line represents the results obtained for neat PVC films.

Table 3 Thermomechanical analyses results for prepared PVC/PhIL/DINP films. The onset degradation temperature (T_{on}), the maximum degradation temperatures of the first weight-loss step (T_p), the temperature at which the films loss 10% of their initial weight ($T_{10\%}$) and the films weight loss at 200 °C were measured by TGA while the films' glass transition temperatures (T_g) and elastic modulus (E') were measured by DMTA. Samples were measured in duplicate with maximum deviations lower than 3% (not shown to simplify data visualization)

Sample	T_{on}[a] (°C)	T_p[b] (°C)	$T_{10\%}$ (°C)	Weight loss at 200 °C (%)	T_g (max tan δ) (°C)	T_g (max E'') (°C)	E' (MPa)		
							−25 °C	0 °C	25 °C
Increasing DINP at fixed incorporated amount of PhIL									
$[P_{14,6,6,6}][Cl]/0.15/0$	180.3	212.0	185.9	19.5	67.8	45.9	2641.5	2300.3	1809.6
$[P_{14,6,6,6}][Cl]/0.15/0.25$	182.1	216.8	188.7	16.2	17.8	−41.8	917.5	317.5	79.1
$[P_{14,6,6,6}][Cl]/0.15/0.50$	191.1	235.7	192.6	13.9	−5.4	−45.8	764.5	165.6	9.6
$[P_{14,6,6,6}][Cl]/0.15/0.75$	202.4	238.9	198.0	11.0	−25.4	−51.5	331.7	27.5	6.2
$[P_{14,6,6,6}][Tf_2N]/0.15/0$	240.5	259.8	235.8	1.7	82.8	−65.2	3059.3	2674.8	2359.6
$[P_{14,6,6,6}][Tf_2N]/0.15/0.25$	254.0	273.0	246.2	1.0	52.9	−36.6	740.9	261.7	79.0
$[P_{14,6,6,6}][Tf_2N]/0.15/0.50$	244.3	276.5	241.9	1.4	−1.5	−47.0	320.9	11.1	3.1
$[P_{14,6,6,6}][Tf_2N]/0.15/0.75$	246.0	275.7	242.2	1.2	−18.3	−49.0	56.8	4.8	0.8
Increasing PhIL at fixed incorporated amount of DINP									
PVC/0/0.15	257.5	271.6	248.1	1.6	63.0	20.7	2392.5	1880.0	1249.9
$[P_{14,6,6,6}][Cl]/0.25/0.15$	178.7	214.3	185.2	17.9	74.8	−32.5	1030.9	278.1	64.1
$[P_{14,6,6,6}][Cl]/0.50/0.15$	177.9	217.5	185.2	16.0	−11.5	−43.3	343.7	42.1	13.3
$[P_{14,6,6,6}][Cl]/0.75/0.15$	180.1	218.7	184.4	16.4	−13.1	−46.1	212.2	21.9	2.2
$[P_{14,6,6,6}][Tf_2N]/0.25/0.15$	250.6	265.3	252.4	0.7	63.6	Phase	1613.9	985.7	573.2
$[P_{14,6,6,6}][Tf_2N]/0.50/0.15$	250.7	269.6	254.6	0.6	72.0	separation[c]	1115.3	735.2	450.7
$[P_{14,6,6,6}][Tf_2N]/0.75/0.15$	249.0	269.1	258.2	0.5	65.5		508.7	338.9	221.4

[a] Refers to the temperature when oxidation of the first weight-loss step begins. [b] Refers to the temperature of the maximum rate of oxidation of the first weight-loss step and corresponds to the peak temperature from DTG curves. [c] A broad E'' profile was observed for these films which indicate the presence of phase immiscibility (see ESI, S2).

amorphicity, by reducing its glass transition temperature (T_g), thus increasing segmental motion of the polymer chains which results in conductivity enhancement.[38,39] The plasticizing efficiencies of the PhILs and DINP mixtures employed were investigated by DMTA, see Table 3 and Fig. 3. The T_g of the films was taken as the value at the maximum of the damping factor curve (tan δ), as usually reported in the literature, and as the maximum of the loss modulus (E''), which is the temperature at which the films initiate the transition from the vitreous to the rubbery state. The results show that, for both PhILs, the T_g of the films significantly decreases when the amount of DINP is increased, for a fixed amount of PhIL. A linear correlation was found between the film T_g (maximum value of tan δ) and the amount of DINP, with correlation coefficients equal to 0.99 and 0.95 for films with a fixed amount of $[P_{14,6,6,6}][Cl]$ and $[P_{14,6,6,6}][Tf_2N]$, respectively (see ESI, S1†). This behaviour was expected, considering the already known PVC plasticizing efficiency of DINP, and does not seems to be influenced by the presence of PhILs.

A different trend was observed for samples loaded with a fixed amount of DINP and increasing amounts of PhILs. In the case of $[P_{14,6,6,6}][Cl]$, the T_g value decreases significantly with increasing amount of $[P_{14,6,6,6}][Cl]$ (up to −13 °C (max tan δ) or −46 °C (max E'')) which demonstrates its high plasticizing capacity. The values of the storage modulus (E') of the films were also found to decrease, as shown for three representative temperatures (−25, 0, 25 °C) in Table 3. On the contrary, with an increase in the amount of $[P_{14,6,6,6}][Tf_2N]$, the T_g of the films (max tan δ), was maintained above 60 °C and a broad peak was observed in the E'' profile, clearly indicating $[P_{14,6,6,6}][Tf_2N]$ PhTf$_2$N–PVC immiscibility (see ESI, S2†). This was confirmed by analysis of the E' profiles, which present a smoother temperature decrease in the temperature range between −75 °C and 50 °C. Moreover, the decrease in E' observed for these films is also lower than that observed for all the other PVC/PhIL/DINP mixtures (Table 3).

Thermomechanical data presented in Fig. 3 also show the influence of each additive (DINP or PhILs) on conformational changes and microscopic deformations of the polymer chains due to molecular rearrangement after inclusion of the additive(s). These rearrangements are known to affect the macroscopic properties of the films, such as their modulus, dielectric constant and thermal expansion coefficient.[39] Fig. 3A and B give the thermomechanical profiles of the films loaded with the maximum amount of DINP and fixed amount of $[P_{14,6,6,6}][Cl]$ and $[P_{14,6,6,6}][Tf_2N]$ respectively, while Fig. 3C and D show the profiles of the films loaded with the maximum amount of $[P_{14,6,6,6}][Cl]$ and $[P_{14,6,6,6}][Tf_2N]$, respectively, for a fixed amount of DINP. In the first case, similar profiles were observed, indicating that the properties of the films are mainly influenced by the presence of DINP. The profiles permit identification of the vitreous to rubber transitions reported in Table 3 and the typical β secondary relaxations, referring to the amorphous phase of PVC, which are detected in the E'' curve as a maximum at ∼−160 °C for both ILs. Nevertheless the curve of tan δ for the sample loaded with $[P_{14,6,6,6}][Tf_2N]$ (sample $[P_{14,6,6,6}][Tf_2N]/0.75/0.15$) presents a broader peak in the profile which may be indicative of partial immiscibility of $[P_{14,6,6,6}][Tf_2N]$ in the mixture.

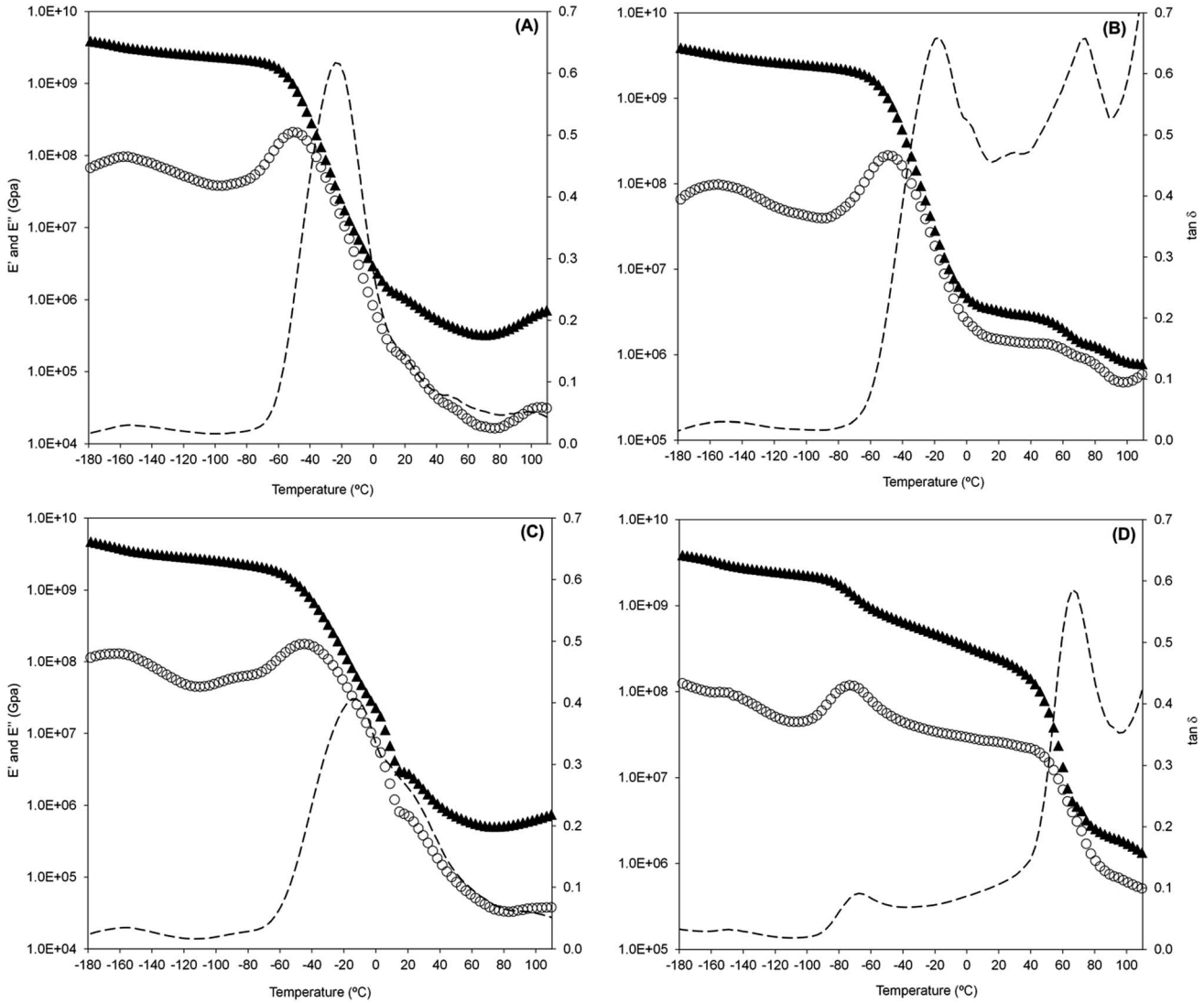

Fig. 3 DMTA thermograms of PVC/DINP/PhIL films at different compositions. The top figures represent the films loaded with the maximum amount of DINP and fixed amount of $[P_{14,6,6,6}][Cl]$, sample $[P_{14,6,6,6}][Cl]/0.15/0.75$ (A) and $[P_{14,6,6,6}][Tf_2N]$, sample $[P_{14,6,6,6}][Tf_2N]/0.15/0.75$ (B). The bottom figures represent the films loaded with fixed amount of DINP and the maximum amount of $[P_{14,6,6,6}][Cl]$, sample $[P_{14,6,6,6}][Cl]/0.75/0.15$ (C) and $[P_{14,6,6,6}][Tf_2N]$, sample $[P_{14,6,6,6}][Tf_2N]/0.75/0.15$ (D). Each figure reports the storage modulus, E' (▲), the loss modulus, E'' (○) and the tan δ curves (– –), for each film.

The higher immiscibility of $[P_{14,6,6,6}][Tf_2N]$ is clearly observed in the second case, at higher PhIL compositions, as observed by the two well-separated T_g values in the tan δ plot (Fig. 3D). The lower of the two T_g at −68 °C can be assigned to a $[P_{14,6,6,6}][Tf_2N]$ rich domain (according to the T_g of the pure $[P_{14,6,6,6}][Tf_2N]$ reported in Table 1) while the higher T_g at 66 °C can be assigned to a PVC rich domain. The incorporation of a higher amount of $[P_{14,6,6,6}][Tf_2N]$ also seems to affect the secondary relaxations of PVC, as reflected in the attenuation of the β relaxation and deviation to a slightly higher temperature. Unlike $[P_{14,6,6,6}][Tf_2N]$, phase immiscibility was not detected in films loaded with higher amounts of $[P_{14,6,6,6}][Cl]$ (Fig. 3C), although the broader tan δ peak reveals that microphase heterogeneity of the $[P_{14,6,6,6}][Cl]$–PVC mixture may start to occur at this composition. These results are in agreement with the SEM images presented and discussed above. Overall, these results indicate a higher $[P_{14,6,6,6}][Cl]$–PVC affinity in comparison with $[P_{14,6,6,6}][Tf_2N]$–PVC systems that present phase segregation at higher incorporated amounts of $[P_{14,6,6,6}][Tf_2N]$. As a consequence, a larger amount of $[P_{14,6,6,6}][Cl]$ can be incorporated into the PVC matrix compared to that of $[P_{14,6,6,6}][Tf_2N]$ (the molar amount of $[P_{14,6,6,6}][Cl]$ is 32% higher than that of $[P_{14,6,6,6}][Tf_2N]$), which also helps to justify its plasticization efficiency.

Impedance spectroscopy

The effect of PhILs and DINP on the electrical resistivity of PVC was investigated by AC impedance spectroscopy and the results are presented in the complex plane impedance plots in Fig. 4A and B. Spectra of PVC films loaded with increasing amounts of

plasticizer, at fixed PhIL composition (Fig. 4A), permit evaluation of the effect of the PVC interchain free volume and polymer chain mobility on charge diffusivity through the polymer matrix and consequently on the conductivity of the polymer. The spectra of PVC films loaded with increasing amounts of PhILs, at fixed plasticizer composition (Fig. 4B), allow evaluation of the effect of the amount of ionic species, cation–anion molecular interactions (ionicity) and anion molar volume on the electrical resistivity of PVC.

The spectra consist of three parts: a first semicircle at high frequencies, a second one at high to intermediate frequencies and capacitive lines at low frequencies. The equivalent circuit used to fit the spectra is shown in Fig. 4C. All spectra contained a cell resistance, R_Ω, at the high frequency intercept comprising the resistances of the two steel electrodes, of the electrical contacts and wires. The values of R_Ω ranged between 3.0 and 10.0 kΩ, for films loaded with fixed DINP composition (0.15 DINP and 0.0–0.75 PhILs) and between 0.7 and 0.9 kΩ for films loaded with fixed PhILs composition (0.15 PhILs and 0.0–0.75 DINP). The first semicircle corresponds to the interfacial impedance and can be represented by a parallel combination of a non-ideal double layer capacitance, CPE_{dl}, and a charge-transfer resistance R_{ct}, while the second semicircle can be attributed to film capacitance and resistance, CPE_f and R_f, respectively. The lower frequency part of the spectra was modelled by a polarisation capacitance, CPE_{pol}, as previously reported.[11] The constant phase element is expressed by $CPE = \{(Ci\omega)^{\alpha}\}^{-1}$, where C is a constant (in this case the capacitance), i is the square root of -1, ω is the angular frequency and α is an exponent which can vary between 1.0 (for uniform and smooth surfaces) and 0.5 (for porous and/or nonhomogeneous surfaces), reflecting the material's non-uniformity and surface roughness.

Table 4 summarizes the values of the circuit elements estimated by fitting the impedance spectra to the equivalent circuit model. The values of R_f, CPE_f and CPE_{pol} were normalized by the thicknesses of the samples (given in Table 2) since this parameter affects the resistance to diffusion of the ionic charges

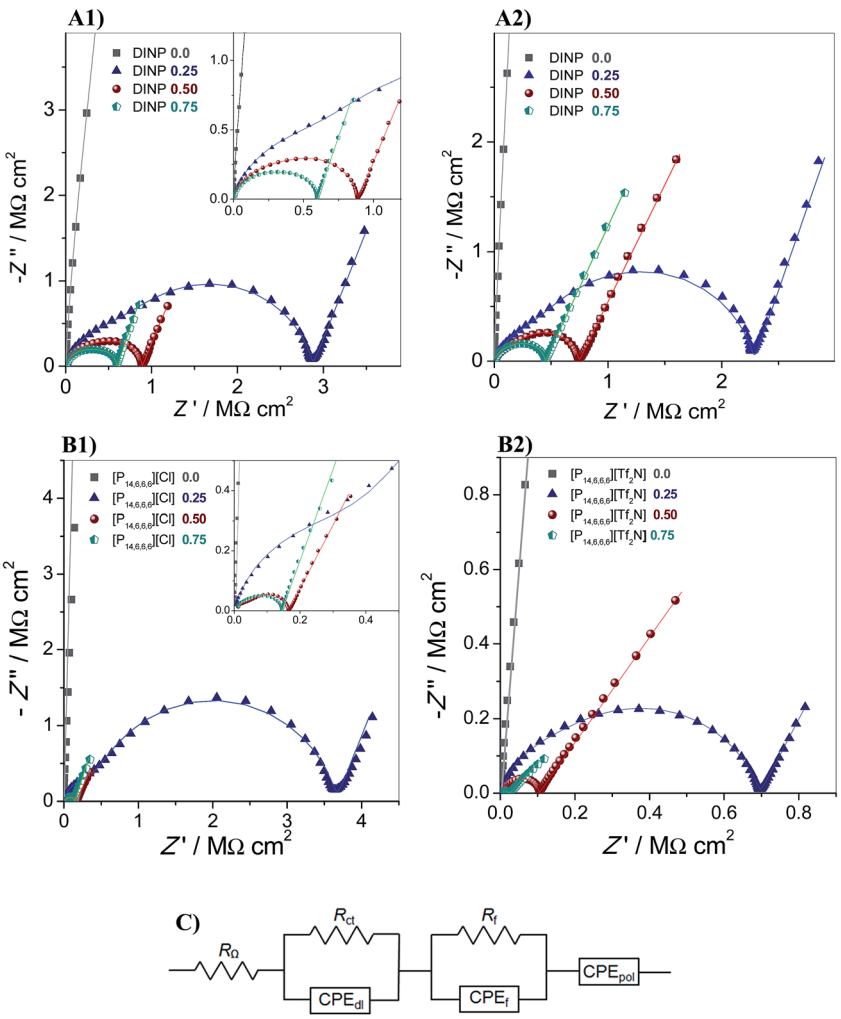

Fig. 4 Complex plane plots recorded for PVC/PhIL/DINP films (A) at fixed PhIL amount and increasing amounts of DINP and (B) at fixed amount of DINP and increasing amounts of PhIL, where 1 = $[P_{14,6,6,6}][Cl]$ and 2 = $[P_{14,6,6,6}][Tf_2N]$; lines show fitting to the electrical equivalent circuit shown in (C).

Table 4 Equivalent circuit element values obtained from fitting the spectra shown in Fig. 4, for PVC films loaded with different amounts of PhILs and DINP. Values for the fitting error are also indicated[a]

Sample	R_{ct} (kΩ cm^2)	CPE_{dl} (pF $s^{\alpha-1}$ cm^{-2})	α_1	ρ_f (MΩ cm)	σ (nS cm^{-1})	CPE_f (pF $s^{\alpha-1}$ cm^{-1})	α_2	CPE_{pol} (pF $s^{\alpha-1}$ cm^{-1})	α_3
Increasing DINP at fixed incorporated amount of PhIL									
$[P_{14,6,6,6}][Cl]$/0.15/0.25	588 (3.1)	87.7 (3.7)	0.87 (0.5)	71.5 (1.6)	14.0	9.84 (2.0)	0.86 (0.8)	60.8 (1.3)	0.76 (0.9)
$[P_{14,6,6,6}][Cl]$/0.15/0.50	322 (5.3)	94.7 (3.1)	0.86 (0.3)	18.1 (4.0)	55.4	6.91 (4.4)	0.92 (1.5)	130.3 (1.0)	0.75 (0.7)
$[P_{14,6,6,6}][Cl]$/0.15/0.75	354 (3.2)	109 (2.9)	0.84 (0.3)	6.4 (6.6)	156	7.18 (6.0)	1.0 (1.1)	210.6 (0.8)	0.79 (0.5)
$[P_{14,6,6,6}][Tf_2N]$/0.15/0.25	410 (5.0)	237 (6.0)	0.82 (0.6)	67.6 (1.2)	14.8	6.93 (6.3)	0.88 (1.0)	36.8 (1.4)	0.79 (1.0)
$[P_{14,6,6,6}][Tf_2N]$/0.15/0.50	188 (3.5)	140 (5.0)	0.84 (0.9)	15.2 (1.4)	65.7	6.84 (5.1)	0.91 (0.8)	65.5 (0.4)	0.72 (0.3)
$[P_{14,6,6,6}][Tf_2N]$/0.15/0.75	174 (2.6)	119 (3.6)	0.84 (0.3)	5.4 (3.2)	182	4.80 (2.8)	0.96 (1.6)	95.9 (0.2)	0.73 (0.2)
Increasing PhIL at fixed incorporated amount of DINP									
$[P_{14,6,6,6}][Cl]$/0.25/0.15	369 (5.9)	66.6 (4.0)	0.92 (0.1)	114 (1.2)	8.8	9.70 (6.3)	0.86 (1.0)	28.7 (2.3)	0.76 (2.4)
$[P_{14,6,6,6}][Cl]$/0.50/0.15	36.1 (3.9)	30 (4.6)	0.97 (0.8)	3.3 (1.3)	303	10.98 (5.1)	0.91 (0.8)	131.8 (0.4)	0.72 (0.3)
$[P_{14,6,6,6}][Cl]$/0.75/0.15	69.0 (6.0)	274 (3.6)	0.8 (0.3)	2.0 (9.0)	511	3.88 (5.8)	0.99 (1.6)	164.1 (0.4)	0.80 (0.3)
$[P_{14,6,6,6}][Tf_2N]$/0.25/0.15	93.0 (7.7)	295 (4.8)	0.85 (0.3)	19.9 (1.2)	50.3	15.7 (3.8)	0.80 (0.2)	213.7 (4.4)	0.70 (4.0)
$[P_{14,6,6,6}][Tf_2N]$/0.50/0.15	33.6 (6.4)	655 (4.0)	0.80 (0.5)	1.8 (1.6)	565	4.53 (6.1)	0.98 (1.0)	143.2 (0.8)	0.64 (0.2)
$[P_{14,6,6,6}][Tf_2N]$/0.75/0.15	17.3 (0.9)	900 (9.0)	0.80 (0.9)	0.4 (5.7)	2356	20 500 (4.0)	0.71 (0.5)	623.2 (0.6)	0.60 (0.5)

[a] Values between parentheses correspond to the fitting error (%). Fitting error = (calculated − experimental)/experimental × 100.

through the polymer matrix. As can be seen in Fig. 4 and by comparing the values in Table 4, a significant reduction of the semicircle diameter at high to medium frequency occurs on increasing the amount of plasticizer (Fig. 4A) and PhIL (Fig. 4B) in the PVC matrix, corresponding to a significant decrease in the resistivity of PVC films. Films loaded with the lowest amounts of DINP or PhILs only, do not significantly affect the insulating nature of PVC (gray square plots in Fig. 4A and B). The spectra recorded for these films were fitted using only a CPE element, with small values between 1 to 5 pF $s^{\alpha-1}$ cm^{-1}, increasing in the order PVC/0/0.15 < $[P_{14,6,6,6}][Tf_2N]$/0.15/0 < $[P_{14,6,6,6}][Cl]$/0.15/0 (values normalized by film thickness).

The effect of the type and amount of the ionic mobile charges near the electrode–PVC film interface can be inferred from R_{ct} values which are significantly higher for films containing fixed and lower PhIL contents (<17 wt%). The lowest R_{ct} values were observed for samples $[P_{14,6,6,6}][Tf_2N]$/0.75/0.15, $[P_{14,6,6,6}][Tf_2N]$/0.50/0.15, and $[P_{14,6,6,6}][Cl]$/0.50/0.15 being 17.3, 33.6 and 36.0 kΩ cm^2, respectively.

The lowest film resistivities (R_f values normalized by the thickness of each film), ρ_f, were obtained for $[P_{14,6,6,6}][Tf_2N]$/0.75/0.15 and $[P_{14,6,6,6}][Cl]$/0.75/0.15, being 0.4 and 2.0 MΩ cm, respectively, indicating a lower resistivity for films loaded with highest PhIL amount (45 wt%). Overall, films incorporating $[P_{14,6,6,6}][Tf_2N]$ had lower resistivity values than those with $[P_{14,6,6,6}][Cl]$. Based on the resistivity of the films, the corresponding conductivity values were determined, as the inverse of resistivity, and the results are presented in Table 4. As expected, the conductivity increases with the amount of both DINP and PhILs, reaching maximum values for $[P_{14,6,6,6}][Tf_2N]$/0.75/0.15 (2.4 μS cm^{-1} at room temperature) which is ~5 times higher than that obtained for $[P_{14,6,6,6}][Cl]$/0.75/0.15 (0.5 μS cm^{-1} at room temperature) and even higher than that obtained for a low PhIL concentration and high amount of DINP plasticizer (0.18 and 0.16 μS cm^{-1}).

Films loaded with the maximum amount of $[P_{14,6,6,6}][Tf_2N]$, at fixed DINP composition, also presented the highest CPE_f and CPE_{pol} values of 20.5 nF $s^{\alpha-1}$ cm^{-1} and 623.2 pF $s^{\alpha-1}$ cm^{-1}, respectively. These values are significantly higher than those observed for all other films which exhibited CPE_f values that were not greatly influenced by the amount of DINP or PhIL (with values between 5 and 15 pF $s^{\alpha-1}$ cm^{-1}) and CPE_{pol} that increased with the amount of DINP or PhILs, similarly to what was previously observed by Dias and co-authors.[11] The higher CPE_{pol} values observed for films loaded with increasing amounts of $[P_{14,6,6,6}][Tf_2N]$ compared to those loaded with $[P_{14,6,6,6}][Cl]$ indicates a higher degree of ion dissociation in the case of $[P_{14,6,6,6}][Tf_2N]$, which enhances the overall ionic conductivity of the solid electrolyte, and suggests that $[P_{14,6,6,6}][Cl]$ diffuses as an anion pair rather than as separate ions in accordance to previously reported data.[4,22–25] This may justify the higher R_f values obtained for films loaded with $[P_{14,6,6,6}][Cl]$ compared to those loaded with $[P_{14,6,6,6}][Tf_2N]$, even if the former was incorporated at a higher molar amount (see above).

Further studies are required to elucidate which of the ions $[P_{14,6,6,6}]^+$ or $[Tf_2N]^-$ plays the main role in increasing the ionic conductivity, knowing that it depends on the molar volume and charge density of the ions but also on the type/strength of the interactions that they may establish with the polymer matrix.[26,28] To our knowledge, there are no reports on the diffusivity of $[P_{14,6,6,6}][Tf_2N]$ confined in solid matrices. Nevertheless, a recent study on the self-diffusion behavior of trihexyltetradecylphosphonium bis(mandelato)borate ($[P_{6,6,6,14}][BMB]$) showed that, in the temperature range between 20 and 50 °C, the cations have lower diffusion coefficients than the anions.[40] Higher mobility of the anion $[Tf_2N]^-$ through the PVC matrix may also result from the chemical repulsions that are likely to exist between the highly electronegative fluorine atoms and chlorine atoms from PVC. Therefore, it may be expected that the anion has a major role in the overall ionic conductivity of the systems studied in the present work.

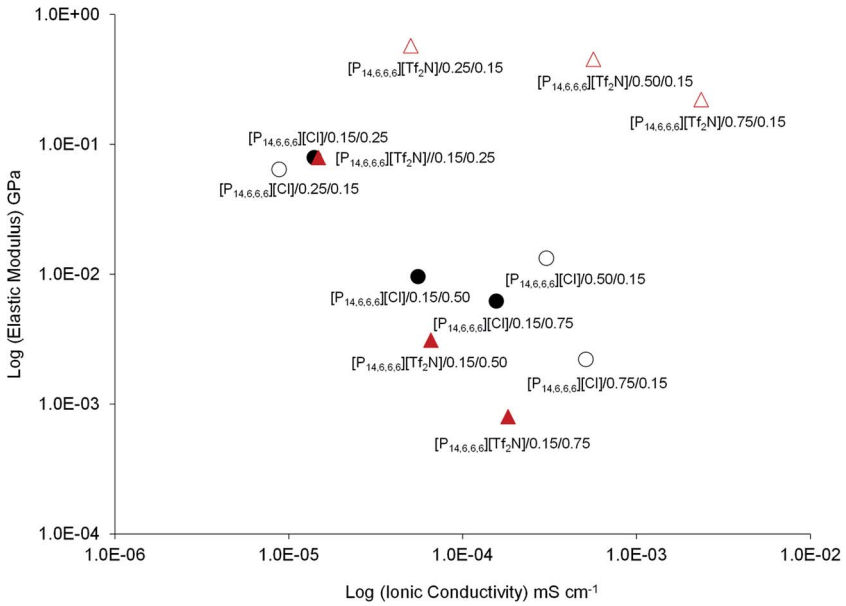

Fig. 5 Multifunctionality graph representing the ionic conductivity and mechanical performance, at room temperature (25 °C), of the PVC–DINP–PhIL materials synthetized in the present work.

Besides electrolyte ionicity, the presence of well-connected conducting channels within the solid matrix may also enhance the ionic conductivity in solid polymer electrolytes. As mentioned above, strong microphase separation occurred in $[P_{14,6,6,6}][Tf_2N]$/PVC films caused by electrolyte–polymer immiscibility. This led to an increase in the tortuosity of the PVC matrix with the formation of conducting micro channel domains through which the free $[P_{14,6,6,6}][Tf_2N]$ ions can preferentially diffuse. This effect may be compared with that of percolation, where conductive fillers are used to produce highly conductive polymer composites based on the conductive tunnelling mechanism.[41] In the case of PVC/$[P_{14,6,6,6}][Tf_2N]$/DINP samples, the percolation threshold occurred for $[P_{14,6,6,6}][Tf_2N]$ compositions higher than 45 wt%.

Finally, an increase in the plasticizer amount at fixed PhIL composition also had an influence on lowering film resistance, although this was not so significant as that observed when increasing the amount of PhIL at fixed plasticizer composition (~3 and 13 times higher for films loaded with $[P_{14,6,6,6}][Tf_2N]$ and $[P_{14,6,6,6}][Tf_2N]$, respectively). The slightly higher increase observed for films loaded with $[P_{14,6,6,6}][Tf_2N]$ compared to $[P_{14,6,6,6}][Tf_2N]$ was expected based on PhIL's ionicity, discussed previously. Therefore, although the presence of a given amount of plasticizer is essential to enhance ionic charge diffusion in between PVC chains,[42] PhIL ionicity and PhIL–PVC interactions are the variables that contribute effectively to a significant increase in the ionic conductivity of the PVC films prepared in this work.

The multifunctionality plot (modulus *vs.* ionic conductivity log–log plot) presented in Fig. 5, shows that a broad range of thermomechanical performances, suitable for different types of application, is covered by the materials presented here. Although these materials present a lower ionic conductivity, than current state of the art values, they are in the range of those previously reported for other RTIL loaded with linear polymers such as poly(ethylene oxide), poly(vinyl alcohol) and poly(-methyl methacrylate).[43] Moreover, it is important to mention that they were obtained using easy-to-apply and scalable procedures, commercially available and relatively low cost materials and without using any ionic conductivity enhancer (such as lithium salts) other than RTILs. This means that further improvements can be anticipated in order to enhance the ionic conductivity of PVC–PhILs based systems. Moreover, PVC films loaded with these additives ($[P_{14,6,6,6}][Tf_2N]$ and DINP) have previously shown[10] excellent biocompatibility as well as negligible leaching of the electrolyte in near physiological condition (ionic strength and temperature) which opens the possibility of using these materials in biomedical engineering applications such as biosensors, bioactuators or electro-responsive drug delivery devices.

Conclusions

Poly(vinyl chloride) (PVC) based ion-conducting films with different ratios of one of two phosphonium ionic liquids ($[P_{14,6,6,6}][Tf_2N]$ or $[P_{14,6,6,6}][Cl]$) and plasticizer (DINP) were prepared. Dynamic mechanical thermal analysis showed that both an increase in the amount of DINP or $[P_{14,6,6,6}][Cl]$ plasticized PVC over the entire temperature range studied, while an increase in the amount of $[P_{14,6,6,6}][Tf_2N]$ led to microphase segregation with the formation of micro channels in-between the PVC molecular chains. The formation of preferential micro channels within the solid matrix together with the higher intrinsic ionicity of $[P_{14,6,6,6}][Tf_2N]$, compared to that of $[P_{14,6,6,6}][Cl]$, justify the significant decrease in the electrical resistivity of PVC films loaded with this RTIL. Moreover, PVC films loaded

with $[P_{14,6,6,6}][Tf_2N]$ and DINP are thermally stable at temperatures up to 200 °C and can therefore be used for applications that require good thermal stability at high temperatures, avoiding the use of PVC thermal stabilizers. Further improvements can, in principle, be achieved by exploring the effect of additional fillers, different PVC grades and different relative phase compositions on the mechanical and electrical performance of these PVC/PhIL based gel polymer electrolytes. Although more studies are still needed, this work demonstrates that PhILs can be used as greener multifunctional electrolytes to produce cheap, stable (thermally, chemically and mechanically) and versatile ionic conducting PVC-based ionic conducting materials.

Acknowledgements

This work was financially supported by Fundação para a Ciência e Tecnologia (FCT-MEC) under contract PTDC/QUI/71398/2006 and PEst-C/EQB/UI0102/2011. A. M. A. Dias and M. M. Barsan acknowledge FCT-MEC for a contract under the program Investigador FCT IF/00455/2013 and the postdoctoral fellowship SFRH/BPD/72656/2010, respectively. H. D. Johansen wishes to thank the Brazilian funding agency Coordenação de Aperfeiçoamento de Pessoal de Nível Superior (CAPES) [BEX 4935/10-1] for the Grants conceded.

References

1 X. Lu, M. Yu, G. Wang, Y. Tong and Y. Li, *Energy Environ. Sci.*, 2014, **7**, 2160.
2 N. Terasawa and K. Asaka, *Sens. Actuators, B*, 2014, **193**, 851.
3 D. R. MacFarlane, N. Tachikawa, M. Forsyth, J. M. Pringle, P. C. Howlett, G. D. Elliott, J. H. Davis, M. Watanabe, P. Simon and C. A. Angell, *Energy Environ. Sci.*, 2014, **7**, 232.
4 R. P. Morco, A. Y. Musa and J. C. Wren, *Solid State Ionics*, 2014, **258**, 74.
5 M. Hayyan, F. S. Mjalli, M. A. Hashim, I. M. AlNashef and T. X. Mei, *J. Ind. Eng. Chem.*, 2013, **19**, 106.
6 S. P. Ong, O. Andreussi, Y. Wu, N. Marzari and G. Ceder, *Chem. Mater.*, 2011, **23**, 2979.
7 M. Smiglak, J. M. Pringle, X. Lu, L. Han, S. Zhang, H. Gao, D. R. MacFarlane and R. D. Rogers, *Chem. Commun.*, 2014, **50**, 9228.
8 D. R. MacFarlane and K. R. Seddon, *Aust. J. Chem.*, 2007, **60**, 3.
9 J. Lu, F. Yan and J. Texter, *Prog. Polym. Sci.*, 2009, **34**, 431.
10 A. M. A. Dias, S. Marceneiro, M. E. M. Braga, J. F. J. Coelho, A. G. M. Ferreira, P. N. Simões, I. M. Veiga, L. C. Tomé, I. M. Marrucho, J. M. S. S. Esperança, A. Matias, C. M. M. Duarte, L. P. N. Rebelo and H. C. de Sousa, *Acta Biomater.*, 2012, **8**, 1366.
11 A. M. A. Dias, A. R. Cortez, M. Barsan, J. B. Santos, C. M. A. Brett and H. C. de Sousa, *ACS Sustainable Chem. Eng.*, 2013, **11**, 1480.
12 M. Ali and T. Hirai, *J. Mater. Sci.*, 2012, **47**, 3777.
13 M. Ali, T. Ueki, D. Tsurumi and T. Hirai, *Langmuir*, 2011, **27**, 7902.
14 H. Xia, T. Ueki and T. Hirai, *Langmuir*, 2011, **27**, 1207.
15 T. Hirai, T. Ogiwara, K. Fuji, T. Ueki, K. Kinoshita and M. Takasaki, *Adv. Mater.*, 2009, **21**, 2886.
16 H. Xia, M. Takasaki and T. Hirai, *Sens. Actuators, A*, 2010, **157**, 307.
17 T. Hirai, H. Xia and K. Hirai, *Proceedings of the 2010 IEEE International Conference on Mechatronics and Automation*, Xian, China, August 4–7, 2010, pp. 71–76, ISBN 978-1-4244-5141-8/10.
18 T. Zhao, Q. Zhou, X. L. He, S. D. Wei, L. Wang, J. M. N. van Kasteren and Y. Z. Wang, *Green Chem.*, 2010, **12**, 1062.
19 D. Glas, J. Hulsbosch, P. Dubois, K. Binnemans and D. E. De Vos, *ChemSusChem.*, 2014, **7**, 610.
20 S. Marceneiro, Q. Hu, A. M. A. Dias, I. Lobo, I. Dias, E. Pinho, M. G. Rasteiro and H. C. de Sousa, *Ind. Eng. Chem. Res.*, 2014, **53**, 16061.
21 F. A. M. M. Goncalves, C. S. M. F. Costa, C. E. Ferreira, J. C. S. Bernardo, I. Johnson, I. M. A. Fonseca and A. G. M. Ferreira, *J. Chem. Thermodyn.*, 2011, **43**, 914.
22 K. J. Fraser, E. I. Izgorodina, M. Forsyth, J. L. Scott and D. R. MacFarlane, *Chem. Commun.*, 2007, 3817.
23 D. R. MacFarlane, M. Forsyth, E. I. Izgorodina, A. P. Abbott, G. Annat and K. Fraser, *Phys. Chem. Chem. Phys.*, 2009, **11**, 4962.
24 O. Holloczki, F. Malberg, T. Welton and B. Kirchner, *Phys. Chem. Chem. Phys.*, 2014, **16**, 16880.
25 K. Ueno, H. Tokuda and M. Watanabe, *Phys. Chem. Chem. Phys.*, 2010, **12**, 1649.
26 A. J. D'Angelo, J. J. Grimes and M. J. Panzer, *J. Phys. Chem. B*, 2015, **119**, 14959.
27 M. W. Schulze, L. D. McIntosh, M. A. Hillmyer and T. P. Lodge, *Nano Lett.*, 2014, **14**, 122.
28 S. A. Chopade, S. So, M. A. Hillmyer and T. P. odge, *ACS Appl. Mater. Interfaces*, 2016, **8**, 6200.
29 N. Shirshova, A. Bismarck, S. Carreyette, Q. P. V. Fontana, E. S. Greenhalgh, P. Jacobsson, P. Johansson, M. J. Marczewski, G. Kalinka, A. R. J. Kucernak, J. Scheers, M. S. P. Shaffer, J. H. G. Steinkef and M. Wienriche, *J. Mater. Chem. A*, 2013, 15300.
30 F. Atefi, M. T. Garcia, R. D. Singer and P. J. Scammels, *Green Chem.*, 2009, **11**, 1595.
31 T. J. Wooster, K. M. Johanson, K. J. Fraser, D. R. MacFarlane and J. L. Scott, *Green Chem.*, 2006, **8**, 691.
32 C. J. Bradaric, A. Downard, C. Kennedy, A. J. Robertson and Y. H. Zhou, *Green Chem.*, 2003, **5**, 143.
33 G. Wypych, *Handbook of Plasticizers*, ed. G. Wypych, ChemTec Publishing, William Andrew Inc., Canada, USA, 2004, p. 36.
34 I. Must, V. Vunder, F. Kaasik, I. Põldsalu, U. Johanson, A. Punning and A. Aabloo, *Sens. Actuators, B*, 2014, **202**, 114.
35 E. Vogler, *Adv. Colloid Interface Sci.*, 1998, **74**, 69.
36 F. S. Majedi, M. M. Hasani-Sadrabadi, S. H. Emami, M. A. Taghipoor, E. Dashtimoghadam, A. Bertsch, H. Moaddel and P. Renaud, *Chem. Commun.*, 2012, **48**, 7744.
37 A. G. M. Ferreira, P. N. Simões, A. F. Ferreira, M. A. Fonseca, M. S. A. Oliveira and A. S. M. Trino, *J. Chem. Thermodyn.*, 2013, **64**, 80.

38 E. Quartarone and P. Mustarelli, *Chem. Soc. Rev.*, 2011, **40**, 2525.
39 D. R. MacFarlane, J. Sun, P. Meakin, P. Fasoulopoulos, J. Hey and M. Forsyth, *Electrochim. Acta*, 1995, **40**, 2131.
40 A. Filippov, F. U. Shah, M. Taher, S. Glavatskih and O. N. Antzutkin, *Phys. Chem. Chem. Phys.*, 2013, **15**, 9281.
41 J. Jin, Y. Lin, M. Song, C. Gui and S. Leesirisan, *Eur. Polym. J.*, 2013, **49**, 1066.
42 M. A. B. H. Susan, T. Kaneko, A. Noda and M. Watanabe, *J. Am. Chem. Soc.*, 2005, **127**, 4976.
43 Y.-S. Ye, J. Rick and B.-J. Hwang, *J. Mater. Chem. A*, 2013, **1**, 2719.